IMAGING METHODS IN RANDOM MEDIA

JAMES G. BERRYMAN

University of California, Lawrence Livermore National Laboratory, P.O.Box 808 L-200, Livermore, CA 94551-9900, USA, E-mail: berryman1@llnl.gov

LILIANA BORCEA

Computational and Applied Mathematics, Rice University, Houston, TX 77005-1892, USA, E-mail: borcea@caam.rice.edu

GEORGE C. PAPANICOLAOU

Department of Mathematics, Stanford University, Stanford, CA 94305, USA, E-mail: papanico@math.stanford.edu

CHRYSOULA TSOGKA

CNRS/LMA, 31 Chemin Joseph Aiguier, 13402 Marseille Cedex 20, FRANCE, E-mail: tsogka@lma.cnrs-mrs.fr

Detection and localization of targets embedded in random media is performed by analysing array data of the scattered field. As the random medium is a source of scattered energy we assume that the targets are more reflective than the background fluctuations so that a clear distinction can be made between targets and background scatterers. We show that the key to successful imaging is finding statistically stable functionals which provide estimates of scatterer locations.

1. Introduction

Imaging in ultrasonics is closely related to recent studies of time-reversal acoustics[8,6]. The work of Prada and Fink [6] and Prada *et al.* [7] on the D.O.R.T. method (diagonalization of the time reversal operator) has clarified the connection between scatterers and the eigenfunctions of the time-reversal operator. After decomposing the array response matrix using eigenfunctions, we can either use the eigenfunctions to refocus acoustic energy back onto the scatterers, or we can use them to form an image of the scatterers' spatial distribution. Both of these applications are relatively straightforward when the background medium is homogeneous [9]. But, if the background medium is heterogeneous, several difficulties arise. Our

focus in this paper concentrates on the difficulties introduced by spatial heterogeneities of the acoustic medium, and on what can be done with acoustic array data to achieve reliable images of scatterers in such media.

There have been many methods of estimating target location using acoustic array data. One of the most popular is matched-field (MF) processing [3,4,5]. We will be discussing here necessary modifications of the MF method, since the randomness we consider has a different character than that usually envisioned in traditional analyses of acoustic array data, because it comes from multipathing that is generated by the random medium.

In the first section, we briefly present the problem to be studied. Section 3 focuses on the standard matched-field functional in frequency domain. This method does *not* provide statistically stable results and, therefore, is not useful for imaging in random media with strong multipathing. Section 4 then shows how the same objective functional may be transformed into the time domain in order to produce statistically stable and, therefore, useful images that localize the target cross-range in a satisfactory manner. Section 5 then goes further to show how range information may be obtained from the time-domain arrival data after careful processing and subsequent averaging of multiple copies of the pertinent singular vectors contained in the multistatic array data. Our conclusions are summarized in Section 6.

2. Problem Statement and Notation

A linear array composed by N transducers, located at $\mathbf{x}_p$, for $p = 1, \ldots, N$, probes an unknown acoustic medium containing M ($M \leq N$) small scatterers by emitting pulses and recording the back-scattered echos. We call the resulting data set response (or transfer) matrix $P(t) = (P_{pq}(t))$, where p and q range over all the array elements. Our goal is to detect and localize the M targets in the random medium.

We assume here that the response matrix in frequency domain $\widehat{P}(\omega)$ is symmetric (but not Hermitian), and this is consistent with our simulations. All of our analysis nevertheless carries over to the non-symmetric case. We introduce the singular value decomposition (SVD) of the response matrix,

$$\widehat{P}(\omega) = \widehat{U}(\omega)\Sigma(\omega)\widehat{V}^H(\omega), \tag{1}$$

where the singular vectors $\widehat{\mathbf{U}}_r(\omega)$, $r = 1, \ldots, N$ of $\widehat{P}(\omega)$ are the columns of $\widehat{U}(\omega)$ and the singular values $\sigma_r(\omega)$ of $\widehat{P}(\omega)$ form the diagonal matrix $\Sigma(\omega)$.

We denote $\widehat{\mathbf{g}}_0(\mathbf{y}^s, \omega)$ the vector observed at the array for a source located at $\mathbf{y}^s$ in a deterministic medium (*i.e.*, a homogeneous medium with the averaged velocity of the random medium c_0). In our simulations, c_0

is constant but it could vary in space, assuming prior knowledge of the environment.

Our simulations assume that $\lambda \leq \ell << a << L$, where λ is the central wavelength, ℓ is the correlation length of the inhomogeneity, a is the array aperture, and L is the distance to the targets from the array. This is the regime where multipathing, or multiple scattering, is significant even when the standard deviation of sound speed fluctuations is only a few percent.

All the formulas are presented in their general form in terms of Green's functions. Thus, these formulas are valid either in 2D or in 3D. Due to the high cost of numerically simulating wave propagation in a random medium, with significant multipathing, we only did 2D simulations up to now.

We solve the wave equation in 2D with a numerical method based on the discretization of the mixed velocity-pressure formulation for acoustics. For the spatial discretization we use a new finite element method [2], which is compatible with mass-lumping techniques (*i.e.*, it leads to explicit time discretization schemes) and for the time discretization we use a centered second order finite difference scheme. In the numerical simulations, we have statistically homogeneous Gaussian random velocity fields generated using a random Fourier series, with constant mean $c_0 = 1.5$km/s, and Gaussian correlation function having correlation length $\ell = 0.3$mm and standard deviation ranging from 1% to 5%. The probing pulse is a Ricker with central frequency $\nu = 3$MHz, the carrier wavelength is $\lambda = 0.5$mm and the aperture of the array is $a = 2.5$mm. The targets, which are soft scatterers, are modeled by small squares (the size of a small one is $\lambda/30 \times \lambda/30$, while the size of a larger one is $\lambda/15 \times \lambda/15$).

3. Matched field – central frequency

We present here a well-known frequency-domain imaging method, the matched-field processing [3,4,5]. We compute $\mathcal{G}^{(j)}_{\rm MF}(\mathbf{y}^s)$ and display the objective functional $\mathcal{R}_{\rm MF}(\mathbf{y}^s)$ (see 2) for a discrete set of points $\mathbf{y}^s$ in the target domain. Examples of MF processing are displayed in Fig. 1.

$$\mathcal{G}^{(j)}_{\rm MF}(\mathbf{y}^s) = \left|\widehat{\mathbf{U}}^H_j(\omega)\widehat{\mathbf{g}}_0(\mathbf{y}^s,\omega)\right|^2, \qquad \mathcal{R}_{\rm MF}(\mathbf{y}^s) = \sum_{j=1}^{M} \frac{\mathcal{G}^{(j)}_{\rm MF}(\mathbf{y}^s)}{\max\limits_{\mathbf{y}^s} \mathcal{G}^{(j)}_{\rm MF}(\mathbf{y}^s)}. \quad (2)$$

When the background medium is homogeneous, the significant singular vectors are linear combinations of $\widehat{\mathbf{g}}_0(\mathbf{y}^t_j,\omega)$, where $\mathbf{y}^t_j$ are the target locations and the MF functional has local maxima at the target locations. But in the case of random media and as the random fluctuations in the velocity increase, there are false peaks and the functional may not peak at

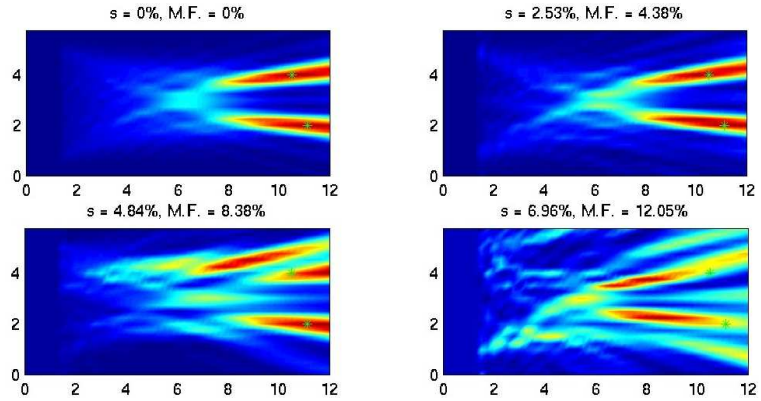

Figure 1. The Matched Field central frequency estimate (2) in random media. The exact location of the targets is denoted by a star. The standard deviation s and maximum fluctuations (M.F.) are indicated on the top of each view. The horizontal axis is the range in mm and the vertical axis is the cross-range in mm.

the targets at all. When the realization of the random medium is changed, the images change also, which is what we call "lack of statistical stability".

4. Matched field in time

We transform here MF into the time-domain to take advantage of the statistical stability that can be gained this way. We compute

$$\mathcal{G}^{(j)}_{\mathrm{MF}_T}(\mathbf{y}^s, t) = \int e^{-i\omega t}\sigma_j(\omega)\left|\widehat{\mathbf{U}}^H_j(\omega)\widehat{\mathbf{g}}_0(\mathbf{y}^s,\omega)\right|^2 d\omega. \tag{3}$$

Since the factor multiplying $e^{-i\omega t}$ in the integrand is real and non-negative, this integral takes its maximum value for $t = 0$. We thus display the following objective functional for points $\mathbf{y}^s$ in the target domain,

$$\mathcal{R}_{\mathrm{MF}_T}(\mathbf{y}^s) = \sum_{j=1}^{M} \frac{\mathcal{G}^{(j)}_{\mathrm{MF}_T}(\mathbf{y}^s, t=0)}{\max\limits_{\mathbf{y}^s} \mathcal{G}^{(j)}_{\mathrm{MF}_T}(\mathbf{y}^s, t=0)}. \tag{4}$$

Examples of MF processing in the time domain are displayed in Fig. 2.

Cross-range results are now dramatically improved. Range information is still not to be found here, but the statistical stability of the "comet tails" is now easily observed. The images shown are for specific realizations, but the results do not change significantly when the underlying realization of the random medium is changed. This fact has been repeatedly shown in our simulations, and is the main characteristic of statistically stable methods.

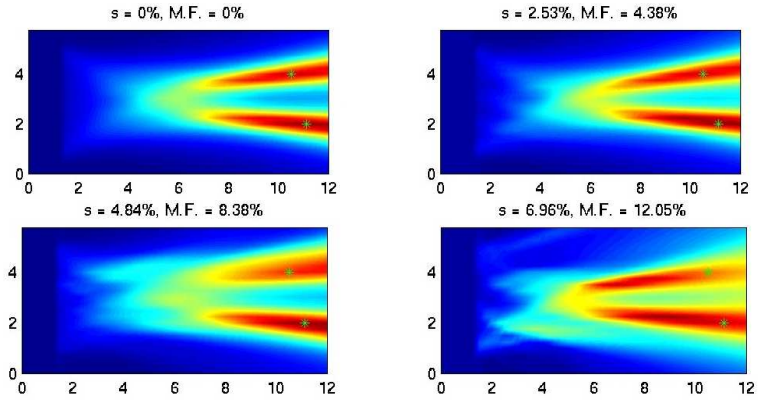

Figure 2. The Matched Field time estimate (4) of the location of two targets in random media. The exact location of the target is denoted by the green star. The standard deviation s and maximum fluctuations (M.F.) are indicated on the top of each view. The horizontal axis is the range in mm and the vertical axis is the cross-range in mm.

5. Time domain processing and range estimation methods

To complete the localization of the targets, we also need an estimate of range. Good range estimates can be obtained in near field either from amplitude move-out information or from arrival time information. In far field, only the arrival time information is useful, and we will concentrate on arrival times in the present analysis.

5.1. *Matched field in time combined with times from averaged singular vectors*

We would like to use the singular vectors $\widehat{\mathbf{U}}_j(\omega)$ to estimate the travel times from target j to the array. Remark though that the singular vectors $\widehat{\mathbf{U}}_j(\omega)$ which are normalized ($\|\widehat{\mathbf{U}}_j(\omega)\| = 1$) carry an arbitrary, frequency dependent, phase. Because of this $\mathbf{U}_j(t)$ look incoherent in the time domain. We can, however, calculate N, coherent in time, versions of singular vectors by projecting the columns of the response matrix onto them

$$\widehat{\mathbf{U}}_j^{(p)}(\omega) = \left[\widehat{\mathbf{U}}_j(\omega)^H \widehat{\mathbf{P}}^{(p)}(\omega)\right] \widehat{\mathbf{U}}_j(\omega),\ p = 1, \ldots, N,\ j = 1, \ldots, M. \qquad (5)$$

Here $\widehat{\mathbf{P}}^{(p)}$ is the p^{th} column of the response matrix $\widehat{P}(\omega)$. Clearly $\widehat{\mathbf{U}}_j^{(p)}(\omega)$ are singular vectors of $\widehat{P}(\omega)$ and carry the phase of its p^{th} column. We use these various versions of the singular vectors to estimate $\tau_p^{(j)}$, for $j = 1, \ldots, M$, and $p = 1, \ldots, N$, the travel times from target j to the array

element p as the minimizers of

$$\min_{\tau_p^{(j)}} \int_0^T \sum_{p=1}^{N} \left| \mathbf{U}_j^{(p)}(t-\tau_p^{(j)}) - \frac{1}{N}\sum_{q=1}^{N} \mathbf{U}_j^{(q)}(t-\tau_q^{(j)}) \right|^2 dt. \tag{6}$$

The ATSV (Arrival Times from averaged Singular Vectors) functional is

$$\mathcal{G}^{(j)}_{\mathrm{ATSV}}(\mathbf{y}^s) = \sum_{p=1}^{N} \left[\tau_p^{(j)} - 2t_p(\mathbf{y}^s)\right]^2, \quad \mathcal{R}_{\mathrm{ATSV}}(\mathbf{y}^s) = \sum_{j=1}^{M} \frac{\min_{\mathbf{y}^s} \mathcal{G}^{(j)}_{\mathrm{ATSV}}(\mathbf{y}^s)}{\mathcal{G}^{(j)}_{\mathrm{ATSV}}(\mathbf{y}^s)}. \tag{7}$$

We combine MF_T with $ATSV$ to obtain

$$\mathcal{R}_{\mathrm{MF}_T\text{-ATSV}}(\mathbf{y}^s) = \sum_{j=1}^{M} \frac{\mathcal{G}^{(j)}_{\mathrm{MF}_T\text{-ATSV}}(\mathbf{y}^s)}{\max_{\mathbf{y}^s} \mathcal{G}^{(j)}_{\mathrm{MF}_T\text{-ATSV}}(\mathbf{y}^s)}, \tag{8}$$

where

$$\mathcal{G}^{(j)}_{\mathrm{MF}_T\text{-ATSV}}(\mathbf{y}^s) = \mathcal{G}^{(j)}_{\mathrm{MF}_T}(\mathbf{y}^s) \,/\, \mathcal{G}^{(j)}_{\mathrm{ATSV}}(\mathbf{y}^s). \tag{9}$$

Examples of $MF_T - ATSV$ estimates are displayed in Fig. 3. This method is statistically stable and gives good estimates of the target locations.

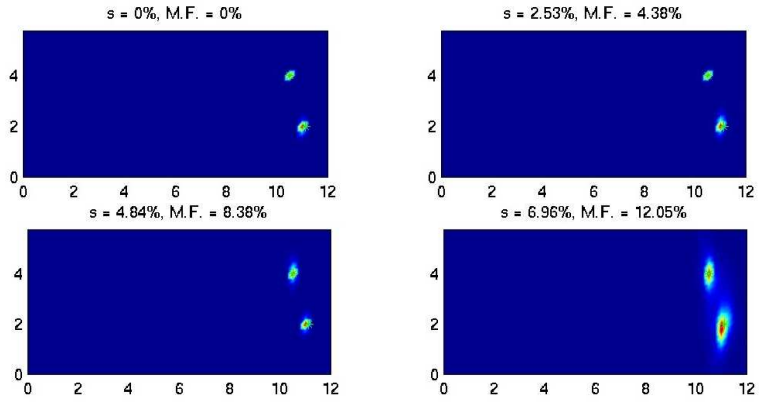

Figure 3. Combined MF_T and $ATSV$ estimation (8) of two targets location in random media. The exact location of the targets is denoted by the green star. The standard deviation s and maximum fluctuations (M.F.) are indicated on the top of each view. The horizontal axis is the range in mm and the vertical axis is the cross-range in mm.

6. Conclusions

For imaging in randomly inhomogeneous media, the foregoing results lead us to the following conclusions: Single frequency methods are not statistically stable, and therefore cannot be used without modification in the presence of significant spatial heterogeneities in the acoustic wave speed. In contrast, time domain methods are statistically stable for any objective functional having the characteristic that the random Green's functions appear in pairs of gg^* [1]. This has been shown here to be true for Matched Field, and is expected to be true more generally[1]. Statistical stability is a necessary, but not a sufficient, condition for optimal imaging in random media, so satisfaction of this criterion is not enough in itself. To locate the targets in random media, we need either multiple views (using multiple arrays) so we can triangulate, or we need to extract a direct measure of range from the data. In the examples chosen here, we concentrated on arrival time and this information was obtained by combining MF with ATSV (arrival times from averaged singular vectors). Another alternative is to use Synthetic Aperture Imaging (SAI) as range estimator[1].

References

1. L. Borcea, G. C. Papanicolaou, C. Tsogka, and J. G. Berryman, "Imaging and time reversal in random media," submitted in *Inverse Problems*.
2. E. Bécache, P. Joly, and C. Tsogka, "An analysis of new mixed finite elements for the approximation of wave propagation problems," *SIAM J. Numer. Anal.* **37**, 1053–1084 (2000).
3. H. P. Bucker, "Use of calculated sound field and matched-field detection to locate sound sources in shallow water," *J. Acoust. Soc. Am.* **59**, 368–373 (1976).
4. A. B. Baggeroer, W. A. Kuperman, and H. Schmidt, "Matched field processing: Source localization in correlated noise as an optimum parameter estimation problem," *J. Acoust. Soc. Am.* **83**, 571–587 (1988).
5. F. B. Jensen, W. A. Kuperman, M. B. Porter, and H. Schmidt, *Computational Ocean Acoustics* (AIP Press, New York, 1994).
6. C. Prada and M. Fink, "Eigenmodes of the time reversal operator: A solution to selective focusing in multiple-target media," *Wave Motion* **20**, 151–163 (1994).
7. C. Prada, S. Manneville, D. Spoliansky, and M. Fink, "Decomposition of the time reversal operator: Detection and selective focusing on two scatterers," *J. Acoust. Soc. Am.* **99**, 2067–2076 (1996).
8. M. Fink, D. Cassereau, A. Derode, C. Prada, P. Roux, M. Tanter, J.-L. Thomas,and F. Wu, "Time-reversed acoustics," *Rep. Prog. Phys.* **63**, 1933–1995 (2000).
9. T. D. Mast, A. I. Nachman, R. C. Waag, "Focusing and imaging using eigenfunctions of the scattering operator," *J. Acoust. Soc. Am.* **102**, 715–725 (1997).